siRNAs targeting terminal sequences of the SARS-associated coronavirus membrane gene inhibit M protein expression through degradation of M mRNA

Zhao-ling Qin, Ping Zhao, Ming-mei Cao, Zhong-tian Qi [*]

Department of Microbiology, State Key Laboratory of Medical Immunology, Second Military Medical University, Shanghai 200433, China

Abstract

SARS-associated coronavirus (SCoV) M protein plays a key role in viral assembly and budding. Recent studies revealed that M protein could interact with N protein in the Golgi complex. In this study, we showed that SCoV M protein co-localized in the Golgi apparatus with a Golgi vector marker. To study M protein function, three candidate small interfering RNAs (siRNAs) corresponding to M gene sequences were designed, transcribed in vitro, and then tested for their ability to silence M protein expression. The plasmid, pEGFP-M, encoding SCoV M protein as a fusion protein with EGFP, was used for silencing and for reporter gene detection in HEK 293T cells transfected with siRNA constructs. The results showed that the mean green fluorescence intensity and M RNA transcripts were significantly reduced, and that the expression of M glycoprotein was strongly inhibited in those cells co-transfected with M-specific siRNAs. These findings demonstrated that the three M-specific siRNAs were able to specifically and effectively inhibit M glycoprotein expression in cultured cells by blocking the accumulation of mRNA, which provides an approach for studies on the functions of M protein and for the development of novel prophylactic or therapeutic agents for SCoV infection.
© 2007 Elsevier B.V. All rights reserved.

Keywords: SARS-associated coronavirus; M glycoprotein; RNA interference; siRNA; Antiviral effect

1. Introduction

Severe acute respiratory syndrome-associated coronavirus (SCoV), a pathogenic agent of human coronaviruses, was identified in April 2003. SCoV, a Group Four coronavirus, is enveloped, with a single-stranded positive-sense RNA genome of about 29,727 nucleotides in length. Based on the sequenced complete SCoV genomes, SCoV encodes at least five major structural proteins: spike (S), envelope (E), membrane (M), nucleocapsid (N) (Peiris et al., 2003; Fouchier et al., 2003; Rota et al., 2003), and the newly identified ORF3a (Shen et al., 2005), which are common to all known coronaviruses. SCoV can cause severe acute respiratory distress syndrome with a diffuse alveolar damage (DAD) at autopsy (Peiris et al., 2003; Kuiken et al., 2003; Nicholls et al., 2003). At present, there is no vaccine or specific effective antiviral method available to treat this disease effectively.

RNA interference (RNAi) is a cellular process in which double-stranded RNA (dsRNA) molecules can silence targeted genes through sequence-specific cleavage of the corresponding RNA transcript. Transfection of small interfering RNAs (siRNAs) into mammalian cells leads to the degradation of the target gene mRNA or to the arrest of protein translation silence of the protein expression (Fire et al., 1998; Elbashir et al., 2001). Therefore, siRNA-mediated RNAi may provide a useful approach to study host cell-virus interactions and to serve as possible therapeutics in virus infection. siRNAs have been employed as therapeutic molecules in human diseases including cancer, neurogenerative diseases and viral infectious diseases (Shi, 2003; Dy kxhoorn et al., 2003). SCoV, as a RNA virus, may also be an ideal target for the study of its biology and therapeutics by RNAi method.

To date, there are a number of published papers showing that siRNA/shRNA (short hairpin RNA) target different regions or genes in the SCoV genome by various siRNA/shRNA generating strategies. RNAase III specific siRNA targeting the RNA dependant RNA polymerase (RDRP), or the S and N genes, could induce specific degradation of SCoV mRNAs in human

* Corresponding author. Tel.: +86 21 25070312; fax: +86 21 25070312.
E-mail address: qizt@smmu.edu.cn (Z.-t. Qi).

cells (Zhu et al., 2004). Synthesized shRNA targeting the N protein (Tao et al., 2005) and RDRP (Lu et al., 2004), could inhibit the expression of target protein, and the latter significantly reducing the plaque forming ability of SCoV in Vero-E6 cells. siRNA targeting the E, M and N proteins (Shi et al., 2005), leader sequence, TRS, 3′-UTR or the S gene (Wu et al., 2005; Qin et al., 2004; Zhang et al., 2004) could effectively inhibit the expression of these targets. Plasmid-derived siRNA targeting to RDRP (Meng et al., 2006; Wang et al., 2004), the leader sequence (B.J. Li et al., 2005; T. Li et al., 2005), and to the non-structural protein 1 (NSP1) could specifically inhibit the expression of target protein and also suppress the replication and propagation of SCoV in cultured Vero E6 cell lines (Ni et al., 2005). The effect of siRNAs/shRNAs probably resulted in global reduction of subgenome synthesis and subsequent protein expression of SCoV. Therefore, to screen more valid siRNAs targets in SCoV genome will be important to provide more information for the development of better SCoV prophylaxis and therapy.

Among the five SCoV structural genes, M gene encodes a glycoprotein 221 amino acids in length, which contains a short amino-terminal ectodomain (residues 1–14), three transmembrane helices (residues 15–37, 50–72 and 77–99) and a 121-amino acid carboxy-terminal endodomain (Voss et al., 2006; Oostra et al., 2006). M protein is the most abundant viral membrane glycoprotein and a key protein in viral assembly and budding through its interaction with N or S proteins (Kuo and Masters, 2002; He et al., 2004). Since SCoV M protein plays a key role in the viral life cycle, experiments were designed to test whether specific siRNAs could inhibit the expression of M protein, which may hold promise for the development of SCoV gene-specific therapeutics.

In this paper, the subcellular distribution of M protein was established in mammalian cells. siRNAs transcribed in vitro were then introduced into the cells expressing the M protein. The results showed that the M protein is mainly located in the Golgi apparatus, and that the specific siRNAs corresponding to SCoV M gene specifically degraded M mRNA, significantly inhibiting M protein expression.

2. Materials and methods

2.1. Construction of plasmids

The 663 base pair fragment of SCoV M gene was synthesized according to the published sequence (GenBank accession no. AY278554). The membrane protein coding region of this fragment spans from nt 26383 to nt 27048 in the full length SCoV genome. This fragment was used as the template to amplify the DNA fragment encoding amino acid residues 1–221 of SCoV M protein by polymerase chain reaction (PCR). The forward primer was 5′-GAATTCGCCACCATGGCAGACAACGGTAC-3′ and the reverse primer was 5′-GGATCCATCTGTACTAGCAAAG-CAATATTGT-3′ (the underlined sequences were EcoRI and BamHI sites, respectively). Forward and reverse primers (final concentration 0.4 μM) and the PrimeSTAR™ HS DNA Polymerase (final concentration 0.025 U/μl, TaKaRa) were used. The PCR conditions were denaturation (98 °C, 10 s), annealing (55 °C, 10 s) and extension (72 °C, 40 s) for 30 cycles. Then the EcoRI–BamHI fragment was inserted into the corresponding multi-cloning site of a eukaryotic expression vector pEGFP-N1 (Clonetech). The resulting plasmid was named pEGFP-M, in which the enhanced green fluorescence protein (EGFP) gene was located downstream of the M gene. Identity of the M gene to the published sequence was confirmed by DNA sequencing (Bioasia Co., Shanghai). Plasmid Golgi/pDsRed-N1, which specifically locates to the Golgi apparatus in mammalian host cells, was kindly provided by Prof. Yuwen Cong (Department of Pathophysiology, Beijing Institute of Radiation Medicine).

2.2. Design and transcription of siRNAs

The siRNAs corresponding to SCoV membrane gene were designed according to Ambion's siRNA guidelines. A scramble siRNA sequence (Wilson et al., 2003) and EGFP siRNA (Cao et al., 2004) were used as negative and positive controls for silencing, respectively. All sequences of the siRNAs were BLAST searched in the National Center for Biotechnology

Table 1
Sequences of template deoxynucleotides for siRNAs used for target genes

Gene targets	Sequences
T7 promoter	5′-TAATACGACTCACTATAGGAGACAGG-3′
EGFP-siRNA	Antisense: 5′-AAGCTGACCCTGAAGTTCATCCCTGTCTC-3′ Sense: 5′-AAGATGAACTTCAGGGTCAGCCCTGTCTC-3′
Scramble siRNA	Antisense: 5′-AACAAGTCTCGTATGTAGTGGCCTGTCTC-3′ Sense: 5′-AACCACTACATACGAGACTTGCCTGTCTC-3′
M-siRNA1	Antisense: 5′-AACGGTACTATTACCGTTGAGCCTGTCTC-3′ Sense: 5′-AACTCAACGGTAATAGTACCGCCTGTCTC-3′
M-siRNA2	Antisense: 5′-AACTCCTGGAACAATGGAACCCCTGTCTC-3′ Sense: 5′-AAGGTTCCATTGTTCCAGGAGCCTGTCTC-3′
M-siRNA3	Antisense: 5′-AACGACAATATTGCTTTGCTACCTGTCTC-3′ Sense: 5′-AATAGCAAAGCAATATTGTCGCCTGTCTC-3′

Note: The eight nucleotides (nt) underlined sequences of template deoxynucleotides for each siRNA are complemented with those of T7 promoter primer. M-siRNA1, M-siRNA2 and M-siRNA3 target to nt 10–28, nt 41–59 and nt 637–655 of SCoV membrane gene, respectively.

Information's (NCBI), and were not found to have significant homology to genes other than the targets. The DNA template (Table 1) used for siRNA transcription was synthesized by Bioasia Co. The oligonucleotide-directed production of siRNAs with T7 RNA polymerase has been described previously (Qin et al., 2004). For each transcription reaction, 300 µM of each oligonucleotide template and T7 promoter primer were mixed and denatured by heating at 95 °C for 2 min. The following was then added to the mixture: 10× Klenow reaction buffer, dNTP mix (Promega, USA), Exo-Klenow (TaKaRa, Dalian) and nuclease-free water. The reaction was incubated at 37 °C for 30 min. The in vitro transcription was performed in 20 µl of transcription mix: 6 µl hybridization solution, 4 µl 5× T7 reaction buffer, 6 µl rNTP mix, 2 µl T7 RNA polymerase and 2 µl nuclease-free water. After incubation at 37 °C for 2 h, sense and antisense RNAs generated in separate reactions were annealed by mixing both transcription reactions and incubating at 37 °C overnight. The concentration of the generated dsRNA was measured by the absorbance at 260 nm in a BioPhotometer (Eppendorf, Germany). S1 nuclease and RNase-free DNase I (TaKaRa) were added to final concentrations of 10 and 1 U/µg of siRNA, respectively, for the digestion of ssRNA and dsDNA. siRNAs were assessed by RNA gel electrophoresis on 2% agarose.

2.3. Purification of siRNAs

One volume of TE-saturated (pH 4.5) phenol:chloroform:isoamyl alcohol (25:24:1) was added to the in vitro transcribed siRNA, and the sample then spun at 13,000 rpm in a microcentrifuge for 10 min. The upper aqueous phase was collected in a fresh tube and mixed with one volume of chloroform:isoamyl alcohol (24:1) and centrifuged at 13,000 rpm for 10 min. The upper, aqueous phase was then mixed with two volumes of ethanol and 0.1 volumes of 3 mmol/l sodium acetate (pH 5.2), and the sample placed on ice for 30 min, followed by centrifugation at 13,000 rpm for 10 min. The pellet was washed with 1 ml of 70% ethanol, and suspended in nuclease-free water for further use. The purity and integrity of siRNAs were checked by agarose gel electrophoresis.

2.4. Cell culture and transfection

Human embryonic kidney (HEK) 293T cells were grown at 37 °C in Dulbecco's modified Eagle's medium (DMEM) (Sigma) containing 10% heat-inactivated fetal bovine serum (Gibco BRL, USA) supplemented with L-glutamine (1 mM), streptomycin (100 µg/ml) and penicillin (100 U/ml). Twenty-four hours prior to transfection, the cells were seeded into 24-well plates at a density of $0.5–2 \times 10^5$ cells per well in fresh medium (500 µl/well) without antibiotics. For the transfection of adherent HEK 293T cells, a total of 0.8 µg of plasmid DNA (pEGFP-M, Golgi/pDsRed-N1) and/or 10 nM of siRNA mixed with Lipofectamine™ 2000 (Invitrogen, CA, USA) were used according to the manufacturer's instructions. The cells were incubated at 37 °C for various times to optimize gene transcription and expression. The expression of M-EGFP and Golgi-RED

fusion proteins were observed directly under an inverted fluorescence microscope.

2.5. Localization of SCoV M protein

Expression of M-EGFP (green) and Golgi-Red (red) in transfected cells was examined with a fluorescence microscope at 24 and 48 h after co-transfection. At 48 h post-transfection, cells on glass cover slips were rinsed with phosphate-buffered saline (PBS), fixed with 4% paraformaldehyde for 20–30 min at 4 °C, and then examined for M protein by confocal microcroscopy. Then the cells were washed with PBS three times and stored in PBS at 4 °C. Images were viewed and collected by confocal fluorescence microscopy (Leica Microsystems Heidelberg GmbH).

2.6. Fluorescence and flow cytometry analyses

Expression of M-EGFP in transfected cells was examined with a fluorescence microscope (Olympus CK40, Japan) at 24, 48, 72 and 96 h after transfection. For flow cytometric analysis of M-EGFP expression, the cells were harvested at 48 h post-transfection and digested with 0.25% trypsin, washed twice with PBS, and then resuspended in PBS to measure the fluorescence using a Becton Dickinson FACScan flow cytometer with filters (emission, 507 nm; excitation, 488 nm). Samples (about 10^6 cells each) were counted and analyzed with CellQuest software, using non-transfected HEK 293T cells as control. The values were calculated as the percentage of the cell population that exceeded the fluorescence intensity of the control cells and the mean fluorescence intensity of this population.

2.7. Reverse transcription (RT) PCR and real-time quantitative PCR

Total RNA from the test and control cells was extracted at 48 h post-transfection using RNAex Reagent (Watson, Shanghai) and digested with RNase-free DNase I (TaKaRa). One microgram of the RNA was then reverse transcribed into cDNA with oligo(dT)$_{15}$ and the avian myeloblastosis virus (AMV) reverse transcriptase XL (TaKaRa) according to manufacturer's recommendations. Reactions without reverse transcriptase were performed in parallel and yielded no PCR products. The primers (forward primer, 5′-TTGGTGCTGTGATCATTCGT-3′; reverse primer, 5′-AAAGCGTTCGTGATGTAGCC-3′) for SCoV M gene were used for the semi-quantitative RT-PCR reaction as follows: denaturation (94 °C, 55 s), annealing (56 °C, 55 s) and extension (72 °C, 1 min) for 20 cycles. Glyceraldehyde-3-phosphate dehydrogenase (GAPDH) was used as an internal control. GAPDH primers (forward primer, 5′-TGGGCTACACTGAGCACCAG-3′; reverse primer, 5′-AAGTGGTCGTTGAGGGCAAT-3′) were synthesized based on the human GAPDH mRNA sequence (GenBank accession no. BC013310). The reaction conditions were as follows: denaturation (94 °C, 50 s), annealing (60 °C, 30 s) and extension (72 °C, 30 s) for 25 cycles. Then real-time quantitative PCR (Lightcycler, Roche) was performed as described (Rajeevan et
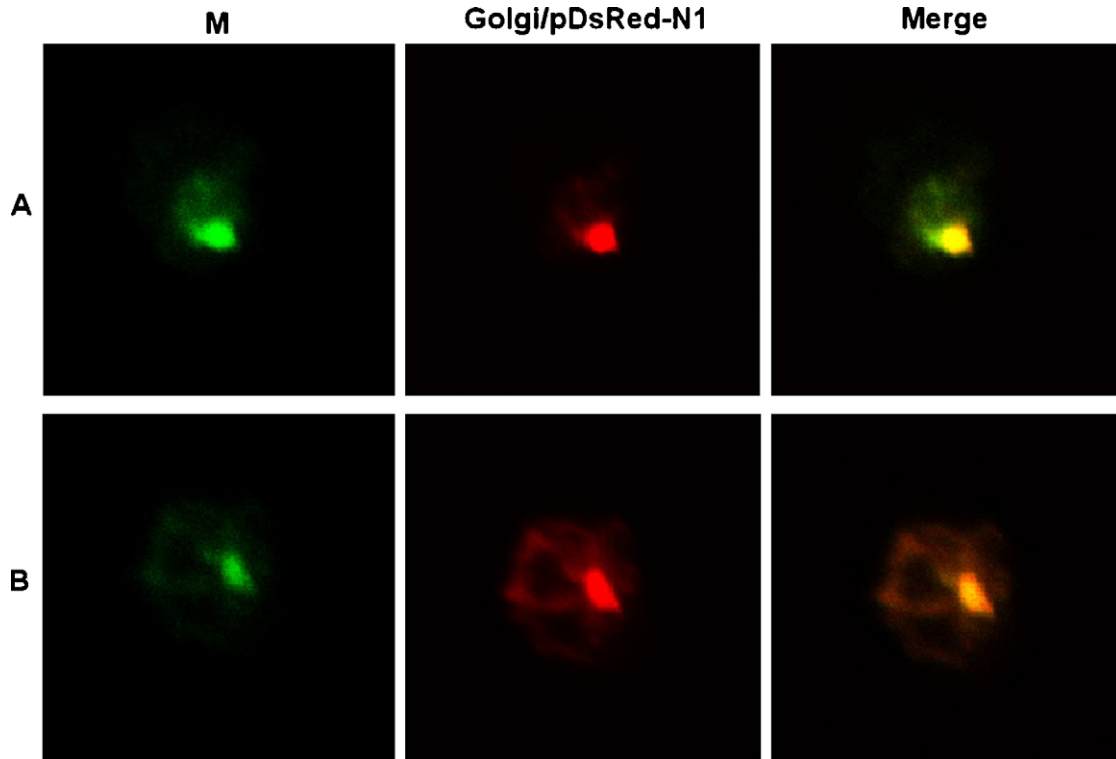
Fig. 1. (A and B) Subcellular co-localization of M-EGFP and Golgi-DsRed protein in HEK 293T cells. The cells were co-transfected with pEGFP-M and Golgi/pDsRed-N1. At 48 h after transfection, cells were fixed and subjected to confocal microscopy.

al., 2001) using SYBR® Premix Ex Taq™ (TaKaRa). Briefly, reactions were carried out in 20 μl volumes containing 2 μl of reverse transcription product. To quantitate SCoV M gene transcript levels, cDNA from the HEK 293T cells transfected with pEGFP-M were diluted in a range from 10^6 to 10^0. For each dilution, amplifications were performed using primers for M and GAPDH genes so that the M mRNA levels could be properly normalized. Each cDNA sample from the transfected HEK 293T cells was run in parallel with the appropriately diluted sample. To perform analysis of relative expression levels of SCoV M gene using real-time PCR, the $2^{-\Delta\Delta CT}$ method was used (Livak and Schmittgen, 2001). The changes of SCoV M gene expression in siRNA co-transfected cells, normalized to GAPDH and relative to its expression in mock-transfected cells, were calculated for each sample. The primers for SCoV M and GAPDH were the same as those described above.

2.8. Western blotting

Cells were harvested and lysed with 1% SDS. Equal amounts of total proteins were separated by 10% sodium dodecyl sulfate-polyacrylamide gel electrophoresis (SDS-PAGE) and electrophoretically transferred to nitrocellulose membrane following the protocol suggested by the manufacturer (Bio-Rad, CA, USA). After blocking non-specific binding sites with 5% non-fat milk, the membrane was incubated with primary antibodies at 4′ overnight. The primary antibodies used were: anti-GFP mouse monoclonal antibody (SantaCruz, 1:500 dilution) and anti-GAPDH mouse monoclonal antibody (KangChen,

Shanghai, 1:5000 dilution). After washing, the blot was incubated with alkaline phosphatase-conjugated goat anti-mouse IgG. Immunoreactive bands were visualized with 5-bromo-4-chioro-3-indolylphosphate/nitroblue tetrazolium (BCIP/NBT) substrate (Sino-American, Shanghai).

3. Results

3.1. Expression and localization of SCoV M glycoprotein in cultured cells

SCoV M gene was cloned into pEGFP-N1 with a C-terminal EGFP tag that could be used to monitor protein expression. At 48 h post-transfection, the fluorescence was mainly in the cytoplasm of HEK 293T cells, where it was condensed into discrete loci and spots (Fig. 1), suggesting that M-EGFP fusion protein was located in a particular cellular compartment. Published data showed that M proteins of other coronaviruses were detectable in the Golgi complex of mammalian cells. At 48 h post-transfection, cells were analyzed by confocal microscopy, which showed that the M-EGFP fusion protein was co-localized in the Golgi apparatus with the Golgi vector marker—Golgi/pDsRed-N1 (Fig. 1). These results suggested that the Golgi distribution of SCoV M protein was conformed, which was also consistent with the previous study (Nal et al., 2005).

3.2. In vitro transcription of siRNAs

To silence the expression of SCoV M glycoprotein using RNAi technology, specific siRNA was made by in vitro tran-
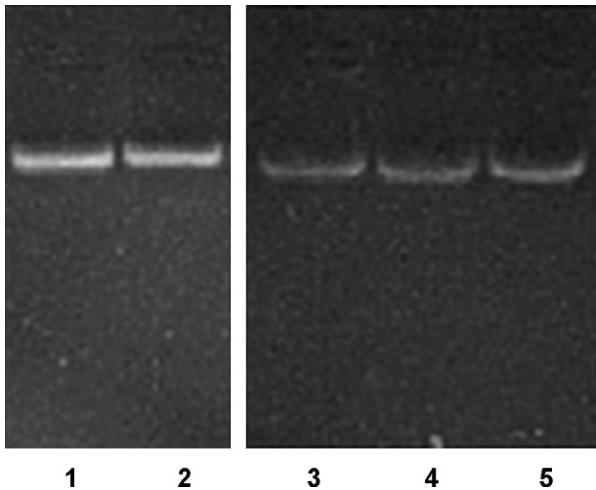
Fig. 2. Purity and integrity of the siRNAs transcribed in vitro. 1. EGFP-specific siRNA. 2. scramble siRNA. 3. SCoV M-siRNA1. 4. SCoV M-siRNA2. 5. SCoV M-siRNA3.

scription. The sense and antisense siRNA templates were separately transcribed in vitro with T7 RNA polymerase and annealed to form double-strand siRNA as described in Section 2. The 5′ overhanging leader sequence of the generated dsRNA and DNA template were digested with single-strand specific nuclease (S1 nuclease) and RNase-free DNase I, respectively. The double stranded siRNAs of 21 nt in length were obtained and found to be intact (Fig. 2).

3.3. Inhibition of membrane gene transcription by siRNAs

Semi-quantitative RT-PCR was performed to examine RNA levels of SCoV M gene in siRNA co-transfected cells. The

data showed that EGFP-siRNA, M-siRNA1, M-siRNA2 and M-siRNA3 reduced the accumulation of M mRNA (Fig. 3A, upper panel, lanes 4, 6, 7 and 8 compared to lane 3), while a control siRNA with scrambled sequence had no effect on M mRNA levels (Fig. 3A, upper panel, lane 5 compared to lane 3) while GAPDH mRNA was not affected by the five siRNAs (Fig. 3A, bottom panel).

To more accurately quantify RNA levels of the SCoV M gene, real-time quantitative PCR was performed using primers specific to the M gene and to GAPDH. cDNA from the HEK 293T cells transfected with pEGFP-M was diluted from 10^6 to 10^0. For each diluted sample, amplifications were performed using primers for the M and GAPDH genes so that the efficiencies of the target and reference genes were similar. Each sample cDNA from the transfected HEK 293T cells was run in parallel with the diluted sample. The change in SCoV M gene expression in siRNA co-transfected cells, normalized to GAPDH and relative to M gene expression in mock-transfected cells, was calculated for each sample using $2^{-\Delta\Delta CT}$ method. The results showed that SCoV M gene mRNA levels were decreased about 45-, 56- and 52-fold in cells transfected with SCoV M-siRNA1, M-siRNA2 and M-siRNA3, respectively, by 48 h post-transfection. Membrane gene transcript levels were decreased about 28-fold in cells transfected with EGFP-siRNA but not significantly changed in cells transfected with control siRNA (Fig. 3B).

3.4. Silencing of SCoV M glycoprotein expression by siRNA

To determine whether siRNA could effectively silence SCoV M glycoprotein expression in cultured cells, pEGFP-M and the various siRNAs were co-transfected into HEK 293T cells. The cells were examined microscopically at 48 h post-transfection for green fluorescence. As shown in Fig. 4, the fluorescence
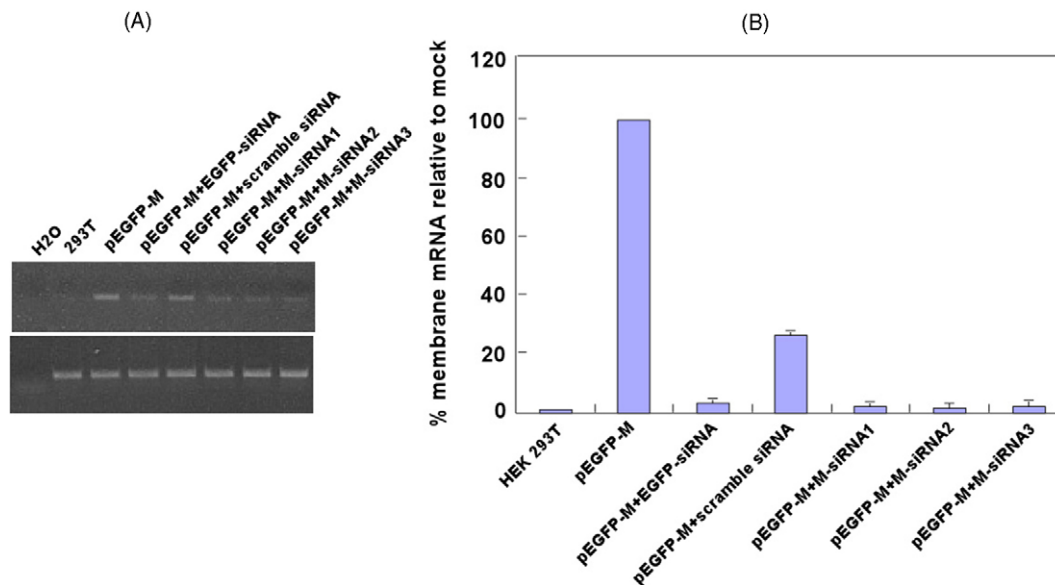

Fig. 3. Reduced SCoV M mRNA in specific siRNAs transfected HEK 293T cells. (A) RT-PCR was performed to show the level of M mRNA in transfected cells. RT-PCR products for the M gene (upper panel) and the internal control, GAPDH (bottom panel), were shown in the figure. (B) Real-time quantitative PCR was performed for the relative quantization of M mRNA on each sample using the $2^{-\Delta\Delta CT}$ method. The assay showed the percentage of SCoV M mRNA in siRNAs transfected HEK 293T cells relative to that in mock-transfected cells. The experiment was repeated for three times and the data were obtained by average. The error bars represent standard error of the mean.
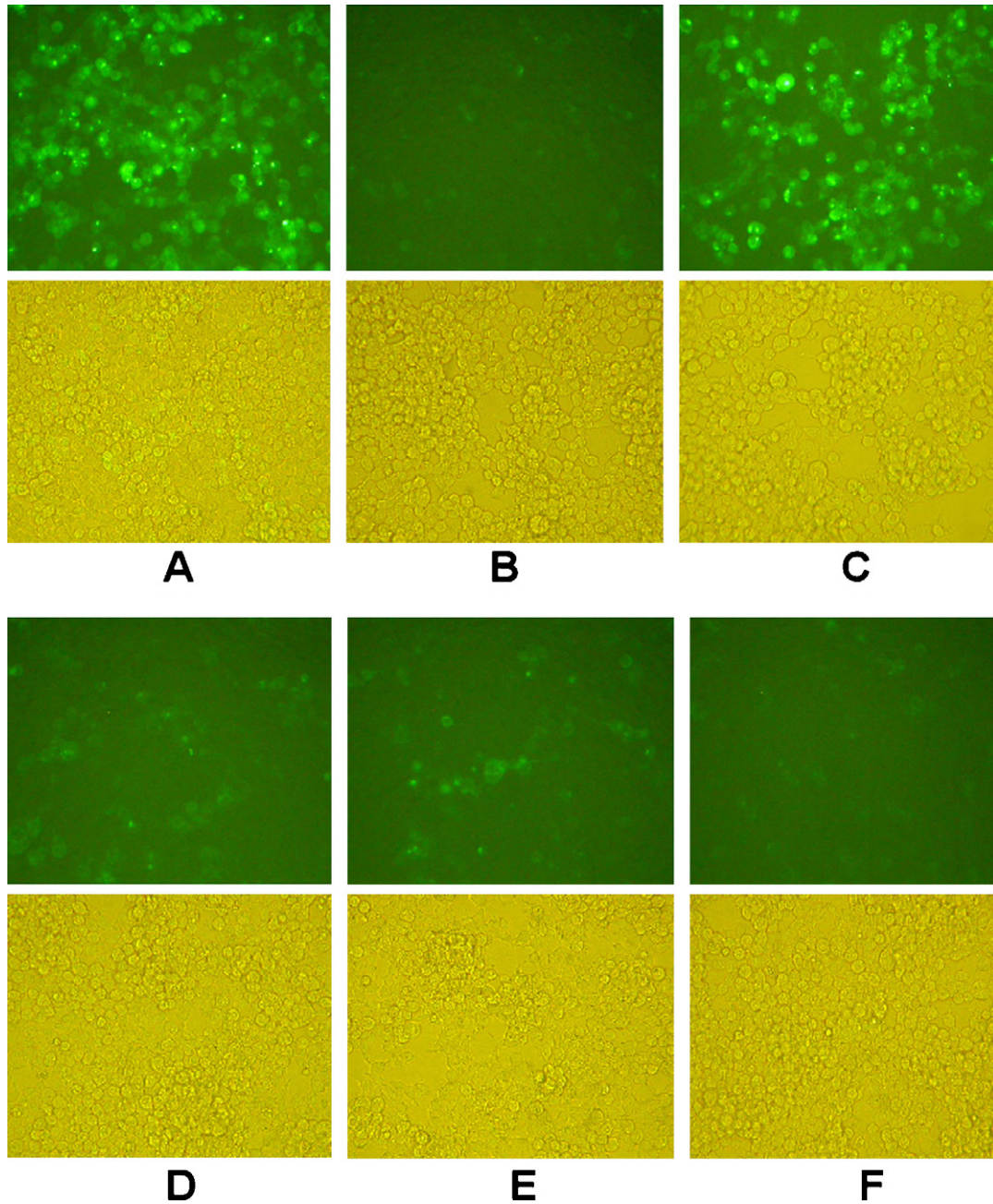
Fig. 4. Effect of siRNAs on the expression of M-EGFP in HEK 293T cells. (A) pEGFP-M transfected. (B) pEGFP-M and EGFP-siRNA co-transfected. (C) pEGFP-M and scramble siRNA co-transfected. (D) pEGFP-M and M-siRNA1 co-transfected. (E) pEGFP-M and M-siRNA2 co-transfected. (F) pEGFP-M and M-siRNA3 co-transfected HEK 293T cells. Upper panels represent the cell fluorescence images recorded at 48 h post-transfection. Bottom panels represent the light microscopic view of cells in the same field. Specific silencing of the M-EGFP fusion protein expression was confirmed in three independent experiments.

image was much stronger in the HEK 293T cells transfected with control siRNA compared to cells transfected with SCoV M-siRNA1, M-siRNA2 and M-siRNA3 (Fig. 4D–F, upper panel). Faint green fluorescence was observed in EGFP-siRNA transfected cells (upper panel B in Fig. 4). The fluorescence intensity of HEK 293T cells co-transfected with control siRNA showed no significant difference from pEGFP-M transfected cells (upper panels A and C in Fig. 4). The bottom panels represent the corresponding image observed by light microscopy. Specific silencing of the green fluorescence was confirmed by at least in three independent experiments.

To further examine the silencing effect of SCoV M-siRNAs, cells were collected and analyzed by fluorescence-activated cell sorting (FACS) 48 h after transfection. Sorting was conducted (using CellQuest software) to select cells that expressed EGFP, using non-transfected HEK 293T cells as a control. As shown in Fig. 5, compared to the cells transfected with plasmid pEGFP-M alone, the cells cotransfected with pEGFP-M and control siRNA gave no significant reduction of EGFP expression, whereas the EGFP-siRNA gave an about 1.9- and 4.3-fold reduction in the percentage of fluorescent cell population and mean fluorescence intensity, respectively. Percentage of fluo-
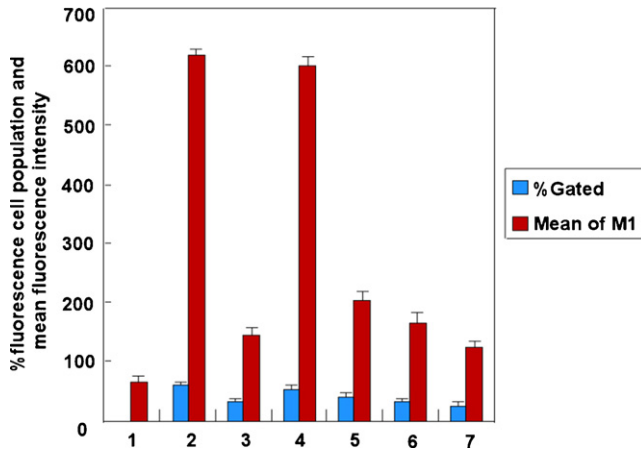
Fig. 5. Flow cytometry analysis of M-EGFP expression in HEK 293T cells. Lanes (1–7) show the results from HEK 293T cells control, cells transfected with pEGFP-M, cells co-transfected with pEGFP-M and EGFP siRNA, cells co-transfected with pEGFP-M and scramble siRNA, cells co-transfected with pEGFP-M and M-siRNA1, cells co-transfected with pEGFP-M and M-siRNA2 and cells co-transfected with pEGFP-M and M-siRNA3, respectively. At 48 h after transfection, cells were analyzed for EGFP expression by flow cytometry. The percentage of the cell population that exceeded the fluorescence intensity of the control cells and the mean fluorescence intensity of this population were calculated. The results represent the means of three independent experiments.

rescence cell population and mean fluorescence intensity were reduced about 1.5- and 3.0-fold for M-siRNA1, 1.9- and 3.7-fold for M-siRNA2 and 2.2- and 5.0-fold for M-siRNA3. This result was in keeping with the fluorescence imaging shown in Fig. 4.

To further determine the effectiveness of siRNA, transfected cells were examined for M-EGFP fusion protein levels in the presence or absence of siRNAs. Western blot analysis showed that compared with the cells transfected with plasmid pEGFP-M alone, M-EGFP fusion protein expression was reduced in cells cotransfected with EGFP-siRNA, M-siRNA1, M-siRNA2 or M-siRNA3, but not reduced in cells cotransfected with control siRNA (upper panel in Fig. 6). Interestingly, a little difference in the level of M-EGFP fusion protein expression in M-siRNA1, M-siRNA2 and M-siRNA3 co-transfected cells was found, indicating that the effect of silencing M-EGFP fusion
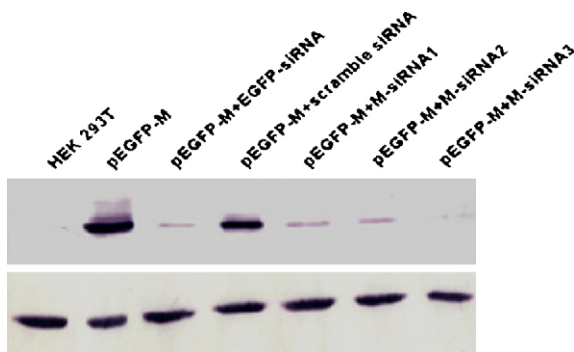

Fig. 6. Effect of siRNA on M-EGFP protein expression in 293T cells. Western blot analysis was performed on equal amounts of proteins harvested from mock- or siRNA-transfected 293T cells at 48 h post-transfection by using GFP- and GAPDH-specific antibodies described in Section 2. GAPDH was used as a loading control.

protein expression by M-siRNA3 was better than M-siRNA1 or M-siRNA2. This was consistent with the data shown in Figs. 4 and 5. GAPDH was not affected by any of the five siRNAs tested (Fig. 6, bottom panel). These data indicate that siRNAs silenced SCoV M glycoprotein expression by blocking the accumulation of M mRNA.

4. Discussions

Individuals with SARS usually develop a high fever followed by severe clinical symptoms. As it is a newly emerging disease, a safe and effective vaccine is not yet available. The role of SCoV M protein in the viral life cycle, especially in viral assembly and budding, makes it an attractive target for anti-SARS drug and vaccine research.

RNAi, induced by double-stranded RNA molecules, can silence target gene expression. Since its discovery in *Caenorhabditis elegans* in 1998, RNAi has been found in many organisms. RNAi could become a reasonable approach in experimental therapeutics for human viral pathogens both in acute and chronic infections (Ketzinel-Gilad et al., 2006). A considerable body of work has demonstrated that RNAi has great prospects in viral therapeutic applications due to its simplicity and specificity compared to many other anti-viral strategies.

Here, the recombinant M-EGFP protein was expressed in HEK 293T cells and spotty fluorescence was found in the transfected cells, which was condensed into discrete loci (Fig. 1). Using confocal microscopy, the results verified that the M-EGFP fusion protein was predominantly located in Golgi compartments (Fig. 1), which is consistent with previous studies (Nal et al., 2005). However, the correct protein band could not be detected by Western blotting analysis when the regular cell lysis buffer (50 mM Tris–Cl, pH 8.0, 150 mM NaCl, 0.02% sodium azide, 1% Triton X-100, 1 μg/ml aprotinin and 100 μg/ml PMSF) was used (data not shown). It was speculated that this failure in detection may be due to its membrane-binding property (Klumperman et al., 1994). Therefore, an alternative method was adopted using 1% SDS to lyse the cells expressing SCoV M protein.

Three candidate M-specific siRNAs were designed and transcribed in vitro to inhibit SCoV M protein. Although siRNAs can be acquired through several methods (Donze and Picard, 2002; Miyagishi and Taira, 2002; Yang et al., 2002; Svoboda et al., 2001; Sui et al., 2002; Lois et al., 2002; Rubinson et al., 2003), transcription in vitro by T7 polymerase is more convenient and reliable than other approaches. Furthermore, the applications of these specifically designed siRNAs, 19–23 nt in length, in animal models have recently made great progress, including the siRNAs targeting Hepatitis B Virus (Xuan et al., 2006), Japanese Encephalitis Virus (Murakami et al., 2005), Human Immunodeficiency Virus (Ping et al., 2004). Based on the extensive screening of the effective siRNAs in vitro, some proper modifications were adopted to improve the efficacy and duration of siRNAs for additional in vivo use. For example, endoribonuclease-prepared siRNAs can efficiently inhibit HBV replication in a mouse model (Xuan et al., 2006), which might be a better therapeutic agent to fight against HBV.

siRNAs have also been pursued for the control of SARS (De Clercq, 2006). Some potent siRNA inhibitors of SCoV in vitro were further evaluated for efficacy and safety in a rhesus macaque SARS model using clinically viable delivery while comparing three dosing regimens. The results showed that specific siRNA could mediate anti-SARS effects either prophylactically or therapeutically, suggesting that a clinical investigation is warranted. This work underscores the prospects for siRNA to enable a significant reduction in development time for new targeted therapeutic agents (B.J. Li et al., 2005; T. Li et al., 2005).

In this study, RT-PCR, real-time quantitative PCR and Western blotting analyses showed that M-siRNA1, M-siRNA2, M-siRNA3 could decrease the SCoV M gene transcript and translational levels compared to the siRNA control (Fig. 3). These data suggested that the effect of gene silencing induced by siRNA should be sequence specific and entire open reading frame (ORF) based. The siRNAs transcribed in vitro can effectively down-regulate SCoV M RNA and protein levels, corresponding to the reported mechanism that siRNAs degrade target mRNA. The resulting three SCoV M specific siRNAs in this study were different from active siRNA reported by other labs (He et al., 2006), suggesting that these effective siRNAs could be further explored as a more efficacious therapeutic agents for SCoV infection.

Previous studies on the M protein revealed that it can interact with N protein (He et al., 2004). In this work, when pEGFP-M was co-transfected with full length SCoV N protein into HEK 293T cells, the fluorescence of recombinant M-EGFP was strongly enhanced (unpublished results). Future work will aim to investigate the mechanism of how SCoV N protein can increase the expression of M protein using specific siRNAs.

Acknowledgements

References

Cao, M.M., Ren, H., Pan, X., Pan, W., Qi, Z.T., 2004. Inhibition of EGFP expression by siRNA in EGFP-stably expressing Huh-7 cells. J. Virol. Methods 119, 189–194.

De Clercq, E., 2006. Potential antivirals and antiviral strategies against SARS coronavirus infections. Expert Rev. Anti Infect. Ther. 4, 291–302.

Donze, O., Picard, D., 2002. RNA interference in mammalian cells using siRNAs synthesized with T7 RNA polymerase. Nucleic Acids Res. 30, e46.

Dyxhoorn, D.M., Novina, C.D., Sharp, P.A., 2003. Killing the message short RNAs that silence gene expression. Nat. Rev. Mol. Cell Biol. 4, 457–465.

Elbashir, S.M., Harborth, J., Lendeckel, W., Yalcin, A., Weber, K., Tuschl, T., 2001. Duplexes of 21-nucleotide RNAs mediate RNA interference in cultured mammalian cells. Nature 411, 494–498.

Fire, A., Xu, S., Montgomery, M.K., Kostas, S.A., Driver, S.E., Mello, C.C., 1998. Potent and specific genetic interference by double-stranded RNA in *Caenorhabditis elegans*. Nature 391, 806–811.

Fouchier, R.A., Kuiken, T., Schutten, M., van Amerongen, G., van Doornum, G.J., vanden Hoogen, B.G., Peiris, M., Lim, W., Stohr, K., Osterhaus, A.D., 2003. Aetiology: Koch's postulates fulfilled for SARS virus. Nature 423, 240.

He, M.L., Zheng, B.J., Chen, Y., Wong, K.L., Huang, J.D., Lin, M.C., Peng, Y., Yuen, K.Y., Sung, J.J., Kung, H.F., 2006. Kinetics and synergistic effects of siRNAs targeting structural and replicase genes of SARS-associated coronavirus. FEBS Lett. 580, 2414–2420.

He, R., Leeson, A., Ballantine, M., Andonov, A., Baker, L., Dobie, F., Li, Y., Bastien, N., Feldmann, H., Strocher, U., Theriault, S., Cutts, T., Cao, J., Booth, T.F., Plummer, F.A., Tyler, S., Li, X., 2004. Characterization of protein–protein interactions between the nucleocapsid protein and membrane protein of the SARS coronavirus. Virus Res. 105, 121–125.

Ketzinel-Gilad, M., Shaul, Y., Galun, E., 2006. RNA interference for antiviral therapy. J. Gene Med. 8, 933–950.

Klumperman, J., Locker, J.K., Meijer, A., Horzinek, M.C., Geuze, H.J., Rottier, P.J., 1994. Coronavirus M proteins accumulate in the Golgi complex beyond the site of virion budding. J. Virol. 68, 6523–6534.

Kuiken, T., Fouchier, R.A., Schutten, M., Rimmelzwaan, G.F., van Amerongen, G., van Riel, D., Laman, J.D., de Jong, T., van Doornum, G., Lim, W., Ling, A.E., Chan, P.K., Tam, J.S., Zambon, M.C., Gopal, R., Drosten, C., van der Werf, S., Escriou, N., Manuquerra, J.C., Stohr, K., Peiris, J.S., Osterhaus, A.D., 2003. Newly discovered coronavirus as the primary cause of severe acute respiratory syndrome. Lancet 362, 263–270.

Kuo, L., Masters, P.S., 2002. Genetic evidence for a structural interaction between the carboxy termini of the membrane and nucleocapsid proteins of mouse hepatitis virus. J. Virol. 76, 4987–4999.

Li, B.J., Tang, Q., Cheng, D., Qin, C., Xie, F.Y., Wei, Q., Xu, J., Liu, Y., Zheng, B.J., Woodle, M.C., Zhong, N., Lu, P.Y., 2005. Using siRNA in prophylactic and therapeutic regimens against SARS coronavirus in Rhesus macaque. Nat. Med. 11, 944–951.

Li, T., Zhang, Y., Fu, L., Yu, C., Li, X., Li, Y., Zhang, X., Rong, Z., Wang, Y., Ning, H., Liang, R., Chen, W., Babiuk, L.A., Chang, Z., 2005. siRNA targeting the leader sequence of SARS-CoV inhibits virus replication. Gene Ther. 12, 751–761.

Livak, K.J., Schmittgen, T.D., 2001. Analysis of relative gene expression data using real-time quantitative PCR and the 2(−Delta Delta C(T)) method. Methods 25, 402–408.

Lois, C., Hong, E.J., Pease, S., Brown, E.J., Baltimore, D., 2002. Germline transmission and tissue-specific expression of transgenes delivered by lentiviral vectors. Science 295, 868–872.

Lu, A., Zhang, H., Zhang, X., Wang, H., Hu, Q., Shen, L., Schaffhausen, B.S., Hou, W., Li, L., 2004. Attenuation of SARS coronavirus by a short hairpin RNA expression plasmid targeting RNA-dependent RNA polymerase. Virology 324, 84–89.

Meng, B., Lui, Y.W., Meng, S., Cao, C., Hu, Y., 2006. Identification of effective siRNA blocking the expression of SARS viral envelope E and RDRP genes. Mol. Biotechnol. 33, 141–148.

Miyagishi, M., Taira, K., 2002. Development and application of siRNA expression vector. Nucleic Acids Res. Suppl., 113–114.

Murakami, M., Ota, T., Nukuzuma, S., Takegami, T., 2005. Inhibitory effect of RNAi on Japanese encephalitis virus replication in vitro and in vivo. Microbiol. Immunol. 49, 1047–1056.

Nal, B., Chan, C., Kien, F., Siu, L., Tse, J., Chu, K., Kam, J., Staropoli, I., Crescenzo-Chaigne, B., Escriou, N., van der Werf, S., Yuen, K.Y., Altmeyer, R., 2005. Differential maturation and subcellular localization of severe acute respiratory syndrome coronavirus surface proteins S, M and E. J. Gen. Virol. 86, 1423–1434.

Ni, B., Shi, X., Li, Y., Gao, W., Wang, X., Wu, Y., 2005. Inhibition of replication and infection of severe acute respiratory syndrome-associated coronavirus with plasmid-mediated interference RNA. Antivir. Ther. 10, 527–533.

Nicholls, J.M., Poon, L.L., Lee, K.C., Ng, W.F., Lai, S.T., Leung, C.Y., Chu, C.M., Hui, P.K., Mak, K.L., Lim, W., Yan, K.W., Chan, K.H., Tsang, N.C., Guan, Y., Yuen, K.Y., Peiris, J.S., 2003. Lung pathology of fatal severe acute respiratory syndrome. Lancet 361, 1773–1778.

Oostra, M., de Haan, C.A., de Groot, R.J., Rottier, P.J., 2006. Glycosylation of the severe acute respiratory syndrome coronavirus triple-spanning membrane proteins 3a and M. J. Virol. 80, 2326–2336.

Peiris, J.S., et al., 2003. Coronavirus as a possible cause of severe acute respiratory syndrome. Lancet 361, 1319–1325.

Ping, Y.H., Chu, C.Y., Cao, H., Jacque, J.M., Stevenson, M., Rana, T.M., 2004. Modulating HIV-1 replication by RNA interference directed against human transcription elongation factor SPT5. Retrovirology 1, 46.

Qin, Z.L., Zhao, P., Zhang, X.L., Yu, J.G., Cao, M.M., Zhao, L.J., Luan, J., Qi, Z.T., 2004. Silencing of SARS-CoV spike gene by small interfering RNA in HEK 293T cells. Biochem. Biophys. Res. Commun. 324, 1186–1193.

Rajeevan, M.S., Vernon, S.D., Taysavang, N., Unger, E.R., 2001. Validation of array-based gene expression profiles by real-time (kinetic) RT-PCR. J. Mol. Diagn. 3, 26–31.

Rota, P.A., Oberste, M.S., Monroe, S.S., Nix, W.A., Campagnoli, R., 2003. Characterization of a novel coronavirus associated with severe acute respiratory syndrome. Science 300, 1394–1399.

Rubinson, D.A., Dillon, C.P., Kwiatkowski, A.V., Sievers, C., Yang, L., Kopinja, J., Rooney, D.L., Ihrig, M.M., McManus, M.T., Gertler, F.B., Scott, M.L., Van Parijs, L., 2003. A lentivirus-based system to functionally silence genes in primary mammalian cells, stem cells and transgenic mice by RNA interference. Nat. Genet. 33, 401–406.

Shen, S., Lin, P.S., Chao, Y.C., Zhang, A., Yang, X.M., Lim, S.G., Hong, W., Tan, Y.J., 2005. The severe acute respiratory syndrome coronavirus 3a is a novel structural protein. Biochem. Biophys. Res. Commun. 330, 286–292.

Shi, Y., 2003. Mammalian RNAi for the masses. Trends Genet. 19, 9–12.

Shi, Y., Yang, D.H., Xiong, J., Jia, J., Huang, B., Jin, Y.X., 2005. Inhibition of genes expression of SARS coronavirus by synthetic small interfering RNAs. Cell Res. Commun. 15, 193–200.

Sui, G., Soohoo, C., Affar el, B., Gay, F., Shi, Y., Forrester, W.C., Shi, Y., 2002. A DNA vector-based RNAi technology to suppress gene expression in mammalian cells. Proc. Natl. Acad. Sci. U.S.A. 99, 5515–5520.

Svoboda, P., Stein, P., Schultz, R.M., 2001. RNAi in mouse oocytes and preimplantation embryos: effectiveness of hairpin dsRNA. Biochem. Biophys. Res. Commun. 87, 1099–1104.

Tao, P., Zhang, J., Tang, N., Zhang, B.Q., He, T.C., Huang, A.L., 2005. Potent and specific inhibition of SARS-CoV antigen expression by RNA interference. Chin. Med. J. (Engl.) 118, 714–719.

Voss, D., Kern, A., Traggiai, E., Eickmann, M., Stadler, K., Lanzavecchia, A., Becker, S., 2006. Characterization of severe acute respiratory syndrome coronavirus membrane protein. FEBS Lett. 580, 968–973.

Wang, Z., Ren, L., Zhao, X., Hung, T., Meng, A., Wang, J., Chen, Y.G., 2004. Inhibition of severe acute respiratory syndrome virus replication by small interfering RNAs in mammalian cells. J. Virol. 78, 7523–7527.

Wilson, J.A., Jayasena, S., Khvorova, A., Sabatinos, S., Rodrigue-Gervais, I.G., Arya, S., Sarangi, F., Harris-Brandts, M., Beaulieu, S., Richardson, C.D., 2003. RNA interference blocks gene expression and RNA synthesis from hepatitis C replicons propagated in human liver cells. Proc. Natl. Acad. Sci. U.S.A. 100, 2783–2788.

Wu, C.J., Huang, H.W., Liu, C.Y., Hong, C.F., Chan, Y.L., 2005. Inhibition of SRAS-CoV replication by siRNA. Antivir. Res. 65, 45–48.

Xuan, B., Qian, Z., Hong, J., Huang, W., 2006. EsiRNAs inhibit hepatitis B virus replication in mice model more efficiently than synthesized siRNAs. Virus Res. 118, 150–155.

Yang, D., Buchholz, F., Huang, Z., Goga, A., Chen, C.Y., Brodsky, F.M., Bishop, J.M., 2002. Short RNA duplexes produced by hydrolysis with *Escherichia coli* RNase III mediate effective RNA interference in mammalian cells. Proc. Natl. Acad. Sci. U.S.A. 99, 9942–9947.

Zhu, X.D., Dang, Y., Feng, Y., Li, T., Huang, P.T., 2004. RNase III-prepared short interfering RNAs induce degradation of SARS-coronavirus mRNAs in human cells. Sheng Wu Gong Cheng Xue Bao 20, 484–489.

Zhang, Y., Li, T., Fu, L., Yu, C., Li, Y., Xu, X., Wang, Y., Ning, H., Zhang, S., Chen, W., Babiuk, L.A., Chang, Z., 2004. Silencing SARS-CoV spike protein expression in cultured cells by RNA interference. FEBS Lett. 560, 141–146.